Earthq Sci (2017) 30(1):57–66
DOI 10.1007/s11589-016-0168-x

RESEARCH PAPER

Study on three independent parameters of focal mechanism solution

Qi Li · Kai Tan

Received: 6 April 2016 / Accepted: 20 September 2016 / Published online: 24 February 2017

Abstract In this paper, the relationships of the plunges and azimuths of *T* and *P* axes versus the strikes, dips, and rakes of two seismic nodal planes were derived to provide reference for earthquake researchers. The independence of the plunges and azimuths of *T*, *B*, and *P* axes in focal mechanism solution was discussed, and it was concluded that three parameters, i.e., the azimuths of *T*, *B* and *P* axes, are completely independent. The focal mechanism solution representation based on Euler rotation was introduced, using three Euler angles in place of the plunges and azimuths of *T*, *B*, and *P* axes, and three focal mechanism solution representations were briefly compared and analyzed in respect of accuracy on the basis of the assumption of rounding; it was concluded that the Euler angle representation has better accuracy, compared with the azimuth representation and the traditional representation with *T*, *B*, and *P* axes.

Keywords Focal mechanism solution · Independence · Euler angels

1 Introduction

As a hot issue in seismological study (Dreger and Helmberger 1990; Ma et al. 1999; Sheng et al. 2015; Gao et al. 2016), the study on the theories and methods for focal mechanism has been widely focused on by the seismologists in China and other countries; China started the study on focal mechanism as early as in the 1950s (Li 1993), and the seismologists have obtained many excellent achievements (Kanamori and Given 1981; Ekström 1989; Okamoto 2002; Zhu and Rivera 2002; Wéber 2006; Kagan 2007; Tape and Tape 2012; Yi et al. 2016). The P-wave first motion method (Reasenberg and Oppenheimer 1985; Hardebeck and Shearer 2002), the P-wave and S-wave amplitude ratio method (Kisslinger et al. 1981; Snoke et al. 1984), and the waveform moment tensor inversion (Dreger and Helmberger 1993; Zhu and Rivera 2002) are common methods to solve for focal mechanism solution at present. Focal mechanism solutions have been applied to the source process (Yue and Lay 2013; Zhang et al. 2013; Zhang et al. 2016) and have become indispensable data for earthquake researchers to carry out study on regional stress fields and seismic hazard assessment (Gephart and Forsyth 1984; Gephart 1990; Arnold and Townend 2007; Martínez et al. 2013; Tan et al. 2016).

Earthquake moment tensor contains relatively complete focal mechanism information. On the basis of the assumption of double-couple point source, information including the strikes, dips, and rakes of seismic nodal planes and the plunges and azimuths of *T*, *B*, and *P* axes can be extracted according to the moment tensor (Knopoff and Randall 1970; Aki and Richards 1980; Jost and Herrmann 1989). To express focal mechanism solution more intuitively, some research institutions such as Global CMT and USGS usually employ the plunges and azimuths of *T*, *B*, and *P* axes and the strikes, dips, and rakes of seismic nodal planes to describe the focal mechanism solution. In fact, these 12 parameters are not independent to each other, for example, based on the strike, dip, and rake of one nodal plane, the strike, dip, and rake of the other nodal plane can be obtained (Ni et al. 1991; Gasperini and Vannucci 2003).

Q. Li · K. Tan (✉)
Key Laboratory of Earthquake Geodetic Surveying, Earthquake Research Institute, China Earthquake Administration, Wuhan 430071, China
e-mail: whgpstan@163.com

In traditional seismology, the P-wave first motion solutions of stations are typically used to invert the strikes, dips, and rakes of two seismic nodal planes, and sometimes to give the plunges and azimuths of T, B, and P axes; when an earthquake is described, the strike, dip, and rake of the earthquake fault often need to be given (Wan et al. 2000). There is universally a paucity of rake data in the focal mechanism solution expression parameters for the historical earthquakes in China (Li 1993); nevertheless, this parameter not only relates to the integrity of the focal coordinate system but also is a key parameter for determining focus type (Aki and Richards 1980). Therefore, it is necessary to find the relationships among 12 parameters of focal mechanism solution, in order to facilitate the use of historical data.

To address the imperfection of traditional earthquake data, Wan et al. (2000) established mathematical relationships of the strikes and dips versus the rakes of two seismic nodal planes, and it is a multi-solution problem. If the parameters of nodal planes of an earthquake are solved for from the plunges and azimuths of T and P axes, no such multisolution problem would exist, but some earthquake researchers might not know the relationships of the plunges and azimuths of T and P axes versus the parameters of two seismic nodal planes and the existing formulas (Krieger and Heimann 2012; Wan 2016; http://epsc.wustl.edu/~ggeuler/codes/m/seizmo/) may not be compact for beginners, leading to many inconveniences in earthquake research efforts. Moreover, to better link up with the traditional seismology, the mathematical relationships among these variables have to be known, so it is very necessary to establish relationships of the plunges and azimuths of T and P axes versus the strikes, dips, and rakes of two seismic nodal planes. T and P axes are perpendicular to each other, maybe someone believe that there are only three independent parameters in solving for the parameters of two seismic nodal planes from the plunges and azimuths of T and P axes, but it is not feasible to extract three completely independent parameters from the plunges and azimuths of any two of T, B and P axes and we have not found systematic discussion about the independence of the plunges and azimuths of T, B and P axis currently (Jost and Herrmann 1989; Snoke 2003; Wan 2016).

Therefore, this paper will try to find a representation alternative to the representation with T, B, and P axes by discussing the independence of the plunges and azimuths of T, B, and P axes and introducing Euler angle, to give three really independent parameters, and to briefly test the accuracy of the independent parameters.

2 Determining strikes, dips, and rakes of two seismic nodal planes based on T and P axes

To facilitate the study, the definitions of the parameters, slip direction, and normal of a seismic nodal plane given by Aki and Richards (1980) were followed in this paper. A rectangular coordinate system was established with the due north direction, the due east direction, and the downward direction perpendicular to ground surface as the positive directions of three coordinate axes, respectively; the geometric relationships among the strike, dip, rake, slip direction, and the normal of nodal plane in this coordinate system are shown in Fig. 1.

Aki and Richards (1980) gave the slip direction $\boldsymbol{x}_1$ and the normal of the nodal plane $\boldsymbol{x}_3$ as follows, respectively,

$$\begin{cases} \boldsymbol{x}_1 = [\sin\lambda\cos\delta\sin\varphi + \cos\lambda\cos\varphi \quad \cos\lambda\sin\varphi - \sin\lambda\cos\delta\cos\varphi \quad -\sin\lambda\sin\delta] \\ \boldsymbol{x}_3 = [-\sin\delta\sin\varphi \quad \sin\delta\cos\varphi \quad -\cos\delta] \end{cases} \tag{1}$$

where $0 \le \varphi \le 2\pi$, $-\pi \le \lambda \le \pi$, and $0 \le \delta \le \pi/2$. Two conjugated seismic nodal planes can be defined from the relationships of the tensional axis and compressional axis versus slip vectors and normal directions (Ni et al. 1991).

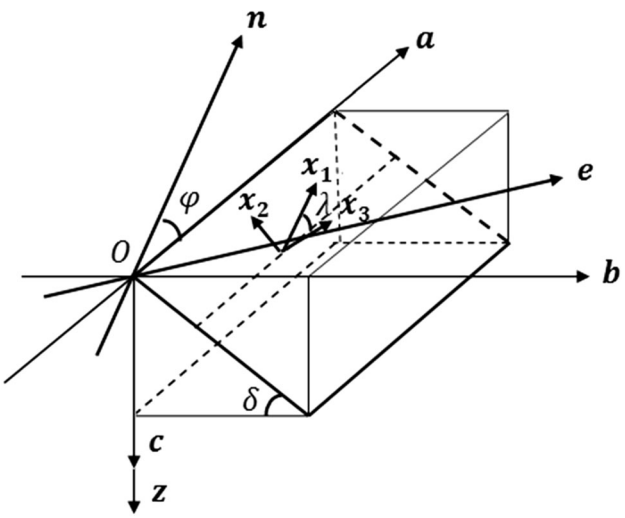

Fig. 1 The definitions of seismic nodal plane parameters, normal, and slip direction. $\boldsymbol{a}$ is the strike of nodal plane; $\boldsymbol{b}$ is the dip direction; $\boldsymbol{e}$ is the due east; $\boldsymbol{n}$ is the due north; $\boldsymbol{x}_1$ is the slip direction; $\boldsymbol{x}_3$ is the normal of nodal plane; $\boldsymbol{c}$ or $\boldsymbol{z}$ is the downward direction perpendicular to ground surface; λ is the rake; δ is the dip

The nodal plane I is

$$\begin{cases} x_1 = \sqrt{2}(\boldsymbol{t} - \boldsymbol{p})/2 \\ x_3 = \sqrt{2}(\boldsymbol{t} + \boldsymbol{p})/2 \end{cases}, \tag{2a}$$

and the nodal plane II is

$$\begin{cases} x_1 = \sqrt{2}(\boldsymbol{t} + \boldsymbol{p})/2 \\ x_3 = \sqrt{2}(\boldsymbol{t} - \boldsymbol{p})/2 \end{cases}, \tag{2b}$$

where $\boldsymbol{p}$ and $\boldsymbol{t}$ are unit vectors of P and T axes, respectively.

The mathematical relationships of the plunges and azimuths of P and T axes versus the strikes, dips, and rakes of two conjugated seismic nodal planes can be established according to Eqs. (1) and (2). From Eq. (1), the following can be obtained:

$$x_{3z} = -\cos\delta. \tag{3a}$$

Since $0 \le \delta \le \pi/2$ and $f(\delta) = -\cos\delta$ is a monotonic function in the interval $[0, 2\pi]$, the dip δ of a nodal plane can be gotten uniquely according to Eq. (3a).

When $\delta \neq 0$ and $\delta \neq \pi/2$, that is, $\sin\delta \neq 0$ and $\cos\delta \neq 0$, the following can be obtained according to Eq. (1):

$$\begin{cases} \cos\varphi = x_{3e}/\sin\delta \\ \sin\varphi = -x_{3n}/\sin\delta \end{cases}, \tag{3b}$$

$$\begin{cases} \sin\lambda = (x_{1e}\cos\varphi - x_{1n}\sin\varphi)/(-\cos\delta) \\ \cos\lambda = x_{1n}\cos\varphi + x_{1e}\sin\varphi \end{cases} \tag{3c}$$

According to Eqs. (3b) and (3c), when $\delta \neq 0$ and $\delta \neq \pi/2$, the strike and rake of one nodal plane can be solved for, respectively.

When $\delta = \pi/2$, the following can be gotten according to Eq. (1):

$$\begin{cases} \cos\varphi = x_{3e} \\ \sin\varphi = -x_{3n} \end{cases}, \tag{3d}$$

$$\begin{cases} \sin\varphi\cos\lambda = x_{1e} \\ \cos\varphi\cos\lambda = x_{1n} \end{cases} \tag{3e}$$

According to Eqs. (3d) and (3e), the strike and rake of a nodal plane when $\delta = \pi/2$ can be solved for, respectively.

When $\delta = 0$, the following can be gotten according to Eq. (1):

$$\begin{cases} \sin\xi = x_{1e} \\ \cos\xi = x_{1n} \end{cases}, \tag{3f}$$

where ξ represents the included angle between the slip direction of nodal plane and the due north direction. The dip angle of the nodal plane is $\delta = 0$, so the strike of the nodal plane is arbitrary and cannot be determined through a mathematical relationship; if it is specified that the slip direction of nodal plane is its strike, then its rake $\lambda = 0$ and its strike $\varphi = \xi$.

Equations (1), (2), and (3) indicate that the strikes, dips, and rakes of two seismic nodal planes can be solved for based on T and P axes. Owing to the orthogonality of T, B, and P axes, this conclusion can be extended to that if the plunges and azimuths of any two of T, B, and P axes are known, then the strikes, dips, and rakes of two nodal planes can be determined accordingly.

It is also known from the equations (1) and (2) that the strike, dip and rake of the other nodal plane can be determined according to the strike, dip and rake of one nodal plane. In this paper, the strike and rake are determined by their sine and cosine values, and the dip is calculated only by its cosine, so it is convenient to be achieved by computer program and easy for beginners to understand. In addition, compared with Wan's method (2016), the method here is simple to determine the dip of seismic nodal plane.

The conclusion was verified with the May 12, 2008 Wenchuan earthquake as an example. According to the moment tensor provided by Global CMT, the plunges and azimuths of T, B, and P axes and the strikes, dips, and rakes of two nodal planes were recalculated and rounded to four decimal places, and the results are listed in Table 1.

3 Independence of plunges and azimuths of T, B, and P axes

The above study shows that the mathematical relationships of the plunges and azimuths of T, B, and P axes versus the parameters of two nodal planes provide an idea for us to determine the rakes. Maybe someone believed that, due to the orthogonality of T and P axes, three independent

Table 1 The focal mechanism solution of Wenchauan earthquake on May 12, 2008

Fault plane 1:	Strike = 231.0039	Dip = 34.7261	Slip = 138.0146
Fault plane 2:	Strike = 357.4924	Dip = 67.6004	Slip = 62.7426
T AXIS:	Plunge: 58.2785	Azimuth: 229.4734	
B AXIS:	Plunge: 25.0515	Azimuth: 8.5996	
P AXIS:	Plunge: 18.1621	Azimuth: 107.4196	

parameters can be extracted from four parameters, namely, the plunges and azimuths of T and P axes, and the three parameters can completely express other nine parameters of focal mechanism solution. But, he neglected the sufficient conditions for the conclusion. Therefore, exploring the independence of the six parameters, i.e., the plunges and azimuths of T, B, and P axes, has some research significance.

Owing to the orthogonal relationships, there are theoretically three independence parameters for the plunges and azimuths of T, B, and P axes, and thus six combinations in total. Assuming that these three axes are denoted by $\boldsymbol{A}_1$, $\boldsymbol{A}_2$ and $\boldsymbol{A}_3$, respectively

$$\begin{cases} \boldsymbol{A}_1 = \cos(pl1)\cdot\cos(az1)\boldsymbol{n} + \cos(pl1)\cdot\sin(az1)\boldsymbol{e} + \sin(pl1)\boldsymbol{z} \\ \boldsymbol{A}_2 = \cos(pl2)\cdot\cos(az2)\boldsymbol{n} + \cos(pl2)\cdot\sin(az2)\boldsymbol{e} + \sin(pl2)\boldsymbol{z} \\ \boldsymbol{A}_3 = \cos(pl3)\cdot\cos(az3)\boldsymbol{n} + \cos(pl3)\cdot\sin(az3)\boldsymbol{e} + \sin(pl3)\boldsymbol{z} \end{cases} \tag{4}$$

3.1 Solve for $az2$ if $pl1$, $az1$, and $pl2$ are known

Since $\boldsymbol{A}_1 \perp \boldsymbol{A}_2$, these following can be obtained from Eq. (4)

$$\cos(pl1)\cos(pl2)\cos(az1 - az2) + \sin(pl1)\sin(pl2) = 0. \tag{5}$$

When $pl1 \neq \pi/2$, $pl2 \neq \pi/2$, Eq. (5) can be written as

$$\cos(az1 - az2) = -\tan(pl1)\tan(pl2). \tag{6}$$

When $\boldsymbol{A}_1$ and $\boldsymbol{A}_2$ are rotating in a plane perpendicular to the horizontal plane, the difference of azimuth between $\boldsymbol{A}_1$ and $\boldsymbol{A}_2$ can reach its maximum $|az1 - az2| = 2\pi$ and minimum $|az1 - az2| = 0$, that is, $0 \le |az1 - az2| \le 2\pi$. Now that $0 \le pl1 \le \pi/2$, $0 \le pl2 \le \pi/2$, so $\cos(az1 - az2) \le 0$, that is, $\pi/2 \le |az1 - az2| \le 3\pi/2$. The value range of function $f(x) = \arccos x$ is $[0, \pi]$, let $\alpha = \arccos[-\tan(pl1)\tan(pl2)]$, so the possible solutions of $az2$ are

$$\begin{cases} az2 = az1 - \alpha \\ az2 = az1 - \alpha + 2\pi \\ az2 = az1 + \alpha \\ az2 = az1 + \alpha - 2\pi \end{cases} \tag{7}$$

It is not difficult to see that the difference between the first and second terms in Eq. (7) is 2π, and the same as the difference between the third and fourth terms. But the difference between the first term and the third or fourth term is not a constant like that between the first and second terms or between the third and fourth terms, so $az2$ has two possible solutions.

The conclusion was verified with the Wenchuan earthquake. Assuming that $\boldsymbol{A}_1$ represents P axis, and $\boldsymbol{A}_2$ represents T axis. Two solutions can be solved for according to Eqs. (6) and (7), and they are 229.4734 and 345.3659, respectively.

As can be discerned from the geometric relationships, the plane where $\boldsymbol{A}_2$ axis is located, that is, the plane represented by ΔOAB in Fig. 2, can be determined according to the plunge $pl1$ and azimuth $az1$, and conical surface where $\boldsymbol{A}_2$ axis is located can be determined according to the plunge $pl2$. The intersecting lines of the plane and the conical surface are the lines where $\boldsymbol{A}_2$ axis is possibly located, so when $pl1 \neq \pi/2$ and $pl2 \neq \pi/2$, $az2$ may has two possible solutions.

3.2 Solve for $az1$, $az2$ and $pl3$ if $pl1$, $pl2$, and $az3$ are known

Since $\boldsymbol{A}_1 \perp \boldsymbol{A}_2$, $\boldsymbol{A}_1 \perp \boldsymbol{A}_3$, and $\boldsymbol{A}_2 \perp \boldsymbol{A}_3$, the following can be obtained from Eq. (4).

When $pl1 \neq 0$ and $pl2 \neq 0$, that is, $pl1 \neq \pi/2$,

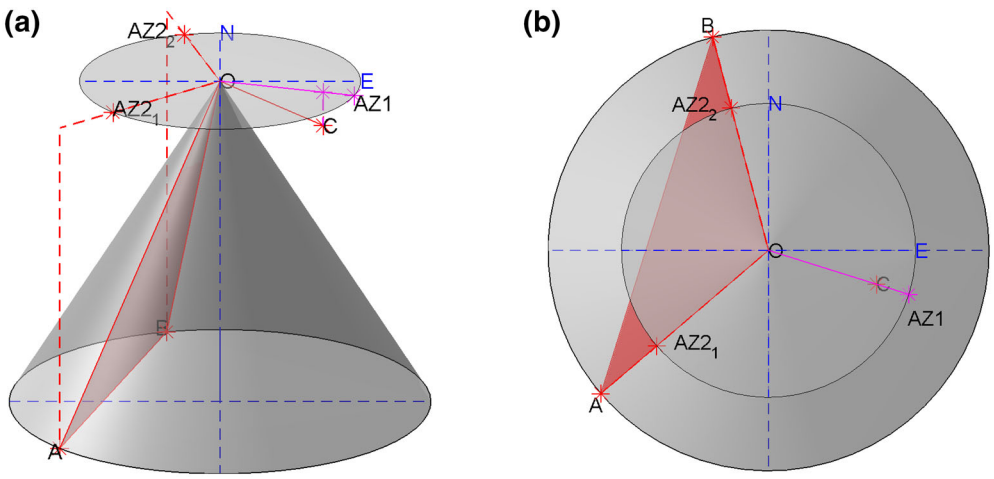

Fig. 2 The azimuthal multiplicity solutions; **a** is the relative positions of azimuthal solutions in three-dimensional space and **b** is its planform. In this case, OC represents the P axis; OA or OB is T axis; AZ1 is the azimuth of P axis; $AZ2_1$ and $AZ2_2$ are two possible azimuths of T axis

$$\tan^2(pl3) = \frac{1 - \tan^2(pl1)\tan^2(pl2)}{\tan^2(pl1) + \tan^2(pl2) + 2\tan^2(pl1)\tan^2(pl2)}. \quad (8)$$

Equation (8) indicates that if the plunges of any two axes are known, then the plunge of the third axis can be determined uniquely. At this moment, let us go back to Sect. 3.1, solve for $az1$ if $pl1$, $pl3$, and $az3$ are known, or solve for $az2$ if $pl2$, $pl3$, and $az3$ are known. As can be discerned from Sect. 3.1, each of $az1$ and $az2$ has two possible solutions, so there are four possible solutions in theory through combination in pairs. However, due to the orthogonality between $\boldsymbol{A}_1$ and $\boldsymbol{A}_2$ axes, there are in fact only two combinations meeting the requirements.

The conclusion was analyzed and verified with the Wenchuan earthquake as an example. Assuming that $\boldsymbol{A}_1$, $\boldsymbol{A}_2$ and $\boldsymbol{A}_3$ axes correspond to T, B, and P axes, respectively, then it can be discerned from Sect. 3.1 that two possible solutions of the plunge of T axis are 229.4734 and 345.3659, respectively, and two possible solutions of the plunge of B axis are 8.5996 and 206.2397, respectively. When the plunges and azimuths of P and T axes are known, the plunges of B axis can be obtained as 8.5996 and 206.2397 according to the orthogonality of P, T, and B axes; similarly, when the plunges and azimuths of P and B axes are known, the plunges of T axis can be obtained as 229.4734 and 345.3659; this indicates that there are in fact only two solutions instead of four solutions.

As can be discerned from the geometric relationships, the plane where $\boldsymbol{A}_1$ and $\boldsymbol{A}_2$ axes are located, that is, the plane represented by ΔOA1A2 in Fig. 3, can be determined according to the plunge $pl3$ and azimuth $az3$ and the conical surfaces where $\boldsymbol{A}_1$ and $\boldsymbol{A}_2$ axes are located can be determined according to the plunges $pl1$ and $pl2$. The intersecting lines of the plane and the conical surface are the lines where $\boldsymbol{A}_1$ and $\boldsymbol{A}_2$ axes are located, and there are two possible lines where each of $\boldsymbol{A}_1$ and $\boldsymbol{A}_2$ axes is located. Owing to the orthogonality between $\boldsymbol{A}_1$ and $\boldsymbol{A}_2$ axes, there are two combinations meeting the requirements, that is, OA1 and OB1, and OA2 and OB2.

3.3 Solve for $pl2$, if $pl1$, $az1$, and $az2$ are known

When $pl1 \neq 0$, $pl2$ satisfies $pl2 \neq \pi/2$; as $\boldsymbol{A}_1 \perp \boldsymbol{A}_2$, the following can be obtained from Eq. (5)

$$\tan(pl2) = -\cos(pl1)\cos(az1 - az2)/\sin(pl1). \quad (9)$$

Since $f(x) = \tan x$ is a monotonic function in the interval $[0, \pi/2]$, the $pl2$ value can be uniquely given according to Eq. (9). Moreover, in view of the geometric relationships, plane I where $\boldsymbol{A}_2$ axis is located can be determined according to the plunge $pl1$ and azimuth $az1$; as $pl1 \neq 0$, plane I is not perpendicular to the horizontal plane; plane II where $\boldsymbol{A}_2$ axis is located can be determined according to the azimuth $az2$, and plane II is perpendicular to the horizontal plane; therefore, between plane I and plane II, there is only one intersecting line, in other words, when $pl1 \neq 0$, the solution of $pl2$ is unique. When $pl1 = 0$, namely, when $\boldsymbol{A}_1$ axis is in the horizontal plane, it can be discerned from Eq. (5) that $\cos(pl2)\cos(az1 - az2) = 0$, so the relationship between $az1$ and $az2$ has to be known before accurately determining the plunge $pl2$ of $\boldsymbol{A}_2$ axis. Analysis from the geometric relationships shows that plane I where $\boldsymbol{A}_2$ axis is located can be determined according to the plunge $pl1$ and azimuth $az1$, and plane II where $\boldsymbol{A}_2$ axis is located can be determined according to the azimuth angle $az2$, and planes I and II are perpendicular to the horizontal plane. When plane I is parallel to plane II, that is, $\cos(az1 - az2) = 0$, which Wan (2016) have not discussed, the plunge $pl2$ has infinite possible values. When plane I is

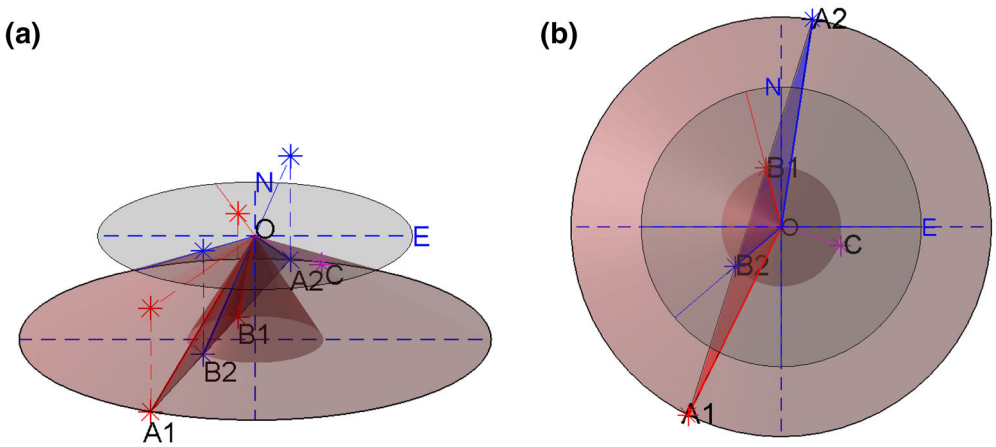

Fig. 3 The azimuthal multiplicity solutions; **a** is the relative positions of azimuthal solutions in three- dimensional space and **b** is its planform. In this case, OC represents the P axis; OA1 or OA2 is the T axis; OB1 or OB2 is the B axis

not parallel to plane II, the $pl2$ value can be uniquely determined, i.e., $pl2 = \pi/2$.

3.4 Solve for $pl1$, $pl2$ and $az3$ if $az1$, $az2$, and $pl3$ are known

Since $\boldsymbol{A}_1 \perp \boldsymbol{A}_2$, $\boldsymbol{A}_1 \perp \boldsymbol{A}_3$, $\boldsymbol{A}_2 \perp \boldsymbol{A}_3$, the following can be gotten from Eq. (4)

$$\cos(\alpha) = c, \tag{10}$$

where $\alpha = az1 + az2 - 2az3, c = -[2\tan^2(pl3)\cos(az1 - az2) + \cos(az1 + az2) + 2\sin(az1)\sin(az2)]$. Since $\pi/2 \le |az1 - az3| \le 3\pi/2$ and $\pi/2 \le |az2 - az3| \le 3\pi/2, 0 \le |az1 + az2 - 2az3| \le 3\pi$, the value range of α should be a subset of $[-3\pi, 3\pi]$, and the possible values of $az3$ can be obtained as follows from Eq. (10)

$$\begin{cases} az3 = (\text{const} - \arccos c)/2 \\ az3 = (\text{const} - \arccos c)/2 - \pi \\ az3 = (\text{const} - \arccos c)/2 + \pi \\ az3 = (\text{const} + \arccos c)/2 \\ az3 = (\text{const} + \arccos c)/2 - \pi \\ az3 = (\text{const} + \arccos c)/2 + \pi \end{cases} \tag{11}$$

Where const = $az1+az2$. In Eq. (11), the difference between the second and third terms is 2π, in other words, the second and third terms represent one angle; similarly, the fifth and sixth terms represent the same angle. Therefore, the number of possible values of $az3$ decreases to 4. The difference between the first and second terms and that between the fourth and fifth terms is π; due to the multi-solution of eigenvector, it can be believed that the first and second terms are equivalent and the fourth and fifth terms are equivalent. Accordingly, $az3$ has two possible solutions.

The conclusion was analyzed and verified with the Wenchuan earthquake as an example. Assuming that $\boldsymbol{A}_1$, $\boldsymbol{A}_2$ and $\boldsymbol{A}_3$ axes correspond to T, B, and P axes, respectively, then the possible solutions of $az3$, $pl1$, and $pl2$ are listed in Table 2.

According to the definition of plunge and Table 2, it can be discerned that $az3$ has two possible solutions and they are the first and second line of Table 2.

Table 2 When $az1$, $az2$, and $pl3$ are known, the possible solutions of $az3$, $pl1$, and $pl2$

$az3$	$pl1$	$pl2$
107.4196	58.2785	25.0515
287.4196	−58.2785	−25.0515
130.6533	25.0515	58.2785
310.6533	−25.0515	−58.2785

3.5 Solve for $pl1$, $pl2$, and $pl3$ if $az1$, $az2$, and $az3$ are known

When $pl1 \neq \pi/2$, $pl2 \neq \pi/2$, and $pl3 \neq \pi/2$, that is, $\cos(az1 - az2) \neq 0, \cos(az1 - az3) \neq 0$ and $\cos(az2 - az3) \neq 0$. Since $\boldsymbol{A}_1 \perp \boldsymbol{A}_2$, $\boldsymbol{A}_1 \perp \boldsymbol{A}_3$, and $\boldsymbol{A}_2 \perp \boldsymbol{A}_3$, the following can be gotten from Eq. (4)

$$\begin{cases} \tan(pl1)\tan(pl2) = -\cos(az1 - az2) \\ \tan(pl1)\tan(\text{pl3}) = -\cos(az1 - az3) \\ \tan(pl2)\tan(pl3) = -\cos(az2 - az3) \end{cases} \tag{12}$$

Let $a = -\cos(az1 - az2)$, $b = -\cos(az1 - az3)$, and $c = -\cos(az2 - az3)$, since $a \neq 0$, $b \neq 0$ and $c \neq 0$, Eq. (12) can be written as

$$\begin{cases} \tan(pl1) = \sqrt{ab/c} \\ \tan(pl2) = \sqrt{ac/b} \\ \tan(pl3) = \sqrt{bc/a} \end{cases} \tag{13}$$

Equation (13) indicates that when $pl1 \neq \pi/2$, $pl2 \neq \pi/2$, and $pl3 \neq \pi/2$, if $az1$, $az2$, and $az3$ are known, then $pl1$, $pl2$, and $pl3$ can be determined uniquely. When $pl1 = \pi/2$, that is, $c = 0$, it follows from Eq. (12) that $\tan(pl2) = 0$ and $\tan(pl3) = 0$, that is, $pl2 = 0$ and $pl3 = 0$. Similarly, when $pl2 = \pi/2$, it follows that $pl1 = 0$ and $pl3 = 0$; when $pl3 = \pi/2$, it follows that $pl1 = 0$ and $pl2 = 0$.

In summary, when $az1$, $az2$, and $az3$ are known, $pl1$, $pl2$, and $pl3$ can be determined uniquely.

3.6 Solve for $az1$, $az2$, and $az3$, if $pl1$, $pl2$, and $pl3$ are known

When $pl1$, $pl2$, and $pl3$ are known, it can be easily discerned according to the geometric relationships that $\boldsymbol{A}_1$, $\boldsymbol{A}_2$ and $\boldsymbol{A}_3$ axes can rotate freely around z axis, in other words, the solutions of $az1$, $az2$, and $az3$ are arbitrary.

The above discussion reveals that there is only one case for the independence of plunges and azimuths of T, B, and P axes in the strict sense, namely, $az1$, $az2$, and $az3$. In practical applications, the case of $pl1$, $az1$, and $az2$ seems feasible, too, and this case can be judged through statistical analysis.

The data of 44,951 earthquakes recorded by Global CMT from January 1, 1976 to December 31, 2015 were obtained, and the plunges and azimuths of T, B, and P axes of every earthquake were recalculated and rounded to four decimal places, based on the moment tensors of these earthquakes. To normalize the requirements, we can let $\boldsymbol{A}_1$ represent T axis and $\boldsymbol{A}_2$ represent P axis, the case that planes I and II are parallel as claimed in Sect. 3.3 can be found according to the recalculation results, for example, for the event 200802140207A, its T axis has plunge

$pl1 = 0$, and azimuth $az1 = 90$, its P axis has plunge $pl2 = 85.0671$ and azimuth $az1 = 0$, and its B axis has plunge $pl3 = 4.9329$ and azimuth $az3 = 180$, so $pl2 + pl3 = 90$, and $az3 - az1 = 90$, in other words, B and P axes are in a plane perpendicular to T axis and horizontal plane. Consequently, the case of $pl1$, $az1$, and $az2$ is not strictly independent. Sections 3.1 and 3.3 correspond to the two cases described by Snoke (2003); the above discussion reveals that it is impossible to completely express 12 parameters of focal mechanism solution by selecting three independent parameters from four parameters, i.e., plunges and azimuths of any two of T, B, and P axes.

3.7 Focal mechanism solution representation based on Euler rotation

In accordance with the Euler's rotation theorem, any two coordinate systems with common origin in a three-dimensional space satisfy that one coordinate system can rotate around a fixed axis containing the origin to the other coordinate system. There are generally three methods to establish connection between these two coordinate systems, namely, quaternion method, rotation matrix method, and Euler angle method, and they can be mutually transformed. The Euler rotation has been widely used in such fields as geoscience and astronautics (Zhu et al. 2010; Wang et al. 2008). When studying on the stress field inversion method, Wan (2015) introduced three Euler angles to express the principal axis of stress tensor based on the Euler's rotation theorem, such that the number of the independent variables of stress tensor decreased from 6 to 4. As T, B, and P axes are eigenvectors of seismic moment tensor and satisfy the relationships of mutual perpendicularity, these three axes can be represented by the same method. According to Wan (2015), the expressions of T, B, and P axes can be let as

$$\begin{cases} \boldsymbol{t} = [\cos\omega_1\cos\omega_3 - \sin\omega_1\cos\omega_2\sin\omega_3 \quad \sin\omega_1\cos\omega_3 + \cos\omega_1\cos\omega_2\sin\omega_3 \quad \sin\omega_2\sin\omega_3] \\ \boldsymbol{p} = [-\cos\omega_1\sin\omega_3 - \sin\omega_1\cos\omega_2\cos\omega_3 \quad -\sin\omega_1\sin\omega_3 + \cos\omega_1\cos\omega_2\cos\omega_3 \quad \sin\omega_2\cos\omega_3] \\ \boldsymbol{b} = [\sin\omega_1\sin\omega_2 \quad -\cos\omega_1\sin\omega_2 \quad \cos\omega_2] \end{cases} \tag{14}$$

where $0 \le \omega_1 \le 2\pi$, $0 \le \omega_2 \le \pi/2$, $0 \le \omega_3 \le \pi$.

From Eq. (14), it is very easy to obtain:

$$\omega_2 = \arccos b_z \tag{15a}$$

When $\omega_2 \neq 0$,

$$\begin{cases} \cos\omega_1 = -b_e/\sin\omega_2,\ \sin\omega_1 = b_n/\sin\omega_2 \\ \cos\omega_3 = p_z/\sin\omega_2,\ \sin\omega_3 = t_z/\sin\omega_2 \end{cases} \tag{15b}$$

When $\omega_2 = 0$,

$$\begin{cases} \boldsymbol{t} = [\cos(\omega_1+\omega_3) \quad \sin(\omega_1+\omega_3) \quad 0] \\ \boldsymbol{p} = [-\sin(\omega_1+\omega_3) \quad \cos(\omega_1+\omega_3) \quad 0] \\ \boldsymbol{b} = [0 \quad 0 \quad 1] \end{cases} \tag{15c}$$

According to Eq. (15c), $\omega_1 + \omega_3$ can be gotten; B axis is perpendicular to the horizontal plane, and T and B axes are in the horizontal plane, so please feel free to let $\omega_3 = 0$, then ω_1 and ω_3 can be determined.

It can be discerned from Eqs. (14) and (15) that T, B, and P axes can be uniquely determined from three Euler rotation angles ω_1,ω_2, and ω_3. Consequently, three Euler angles can be used to independently describe focal mechanism solution.

The above discussion reveals that there are two simple methods that can completely express focal mechanism solution; one is to use the azimuths $az1$, $az2$, and $az3$ to describe focal mechanism solution, and the other is to use three Euler angles ω_1, ω_2 and ω_3 in place of T, B, and P axes. No matter which method is used, if it is wanted to completely recover the original focal mechanism solution information, it relates to accuracy. The research results published generally follow the principle of rounding, and if it is wanted to completely recover original information, avoiding the error caused by artificial rounding, it is very necessary to explore the accuracy of these two methods. 1000 out of 44,951 earthquakes recorded by Global CMT from January 1, 1976 to December 31, 2015 were randomly sampled, the strikes, dips, and rakes of two nodal planes, as well as the plunges and azimuths of T, B, and P axes were recalculated according to the moment tensor of every earthquake, and corresponding Euler angles were solved for. The strikes, dips and rakes of the seismic nodal planes are calculated when the plunges, azimuths and Euler angles are rounded and then do the difference with the original values. Finally, the results are shown in Fig. 4.

It is not difficult to find from Fig. 4 that, in the traditional focal mechanism representation (Fig. 4i–k), after the plunges and azimuths of T and P axes are rounded, if it is wanted to recover complete focal mechanism solution, relatively large error is likely introduced in quite a lot of cases, which is consistent with the research result obtained by Wang (2012). If new representation is used, when the

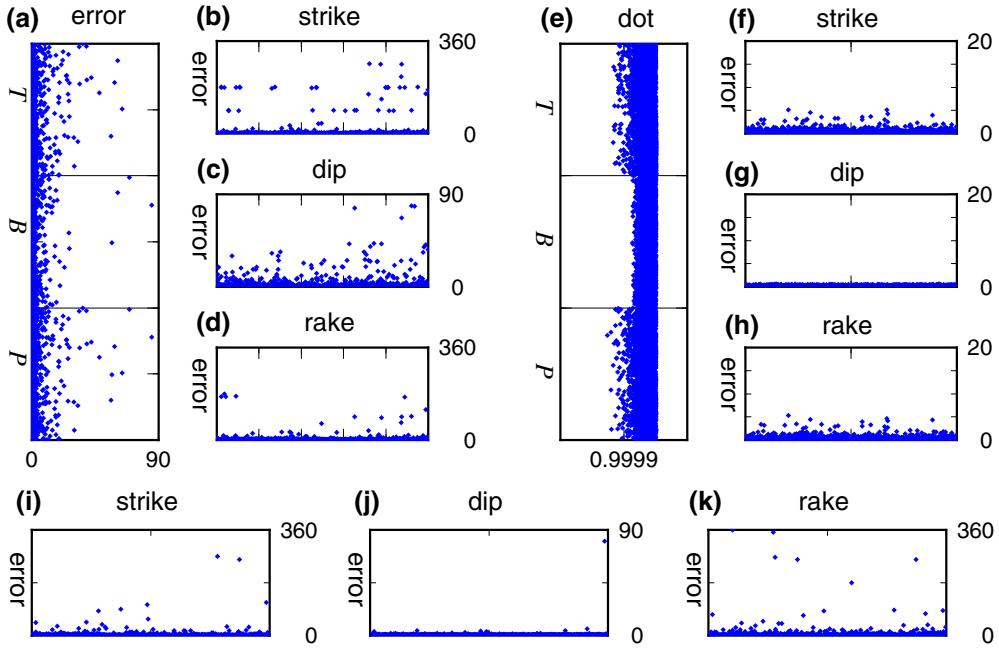

Fig. 4 The errors caused by rounded plunges, azimuths and Euler angles. **a**, **b**, **c**, and **d** are the deviations of plunge, strike, dip, and rake when we round the three azimuths; the *dot* products between the new and old tension axis, compression axis, and neutral axis are show in (**e**) when we round the euler angles and the errors of the strike, dip, and rake are show in (**f**), (**g**), and (**h**), respectively. If we round the azimuths and plunges of two axes, the deviations of strike, dip, and rake are shown in (**i**), (**j**), and (**k**)

azimuths of *T*, *B*, and *P* axes are used to independently express focal mechanism solution (Fig. 4a–d), relatively large error is typically introduced in recovering the original focal mechanism solution information, and the obtained results even completely deviates from the original results, due to rounding; the reason may be that, to solve for the parameters of nodal planes of an earthquake according to the azimuths of three axes, one needs to solve for the plunges of these three axes first, which causes error accumulation. When Euler angles are used to independently express focal mechanism solution (Fig. 4e–h), although Euler angles are rounded, the original focal mechanism information can still be recovered relatively accurately, with the error ranges of azimuth, dip, and rake being limited within 4°; in particular, the error range of the dip angle of nodal plane is not more than 1°, and the errors of the rake and strike are mostly distributed within 1°. This indicates that the method using Euler angles to express focal mechanism solution is better than that using azimuths and is very good supplement to the independence of the plunges and azimuths of *T*, *B*, and *T* axes.

4 Conclusions

In this paper, we derived the detailed and simple formulas for determining the strikes, dips and rakes of the seismic nodal planes based on the plunges and azimuths of any two of *T*, *B* and *P* axes on the basis of previous research results. Owing to the orthogonality of *T*, *B* and *P* axes, there are only three independent parameters in theory. However, through discussion of six combinations of the plunges and azimuths of *T*, *B* and *P* axes, we found that there is only one case for the independence of the plunges and azimuths of *T*, *B* and *P* axes in the strict sense, that is, the azimuths $az1$, $az2$ and $az3$ of three axes, according to which other nine parameters of focal mechanism solution can be uniquely determined.

In addition, on the basis of the assumption of rounding, it was found that solving for other parameters according to the azimuths $az1$, $az2$ and $az3$ of three axes typically induces very large errors; when the parameters of a seismic nodal plane are solved for with the plunges and azimuths of *T* and *P* axes, some solutions have relatively large deviations, too; when three Euler angles are used in place of six parameters, i.e., the plunges and azimuths of *T*, *B* and *P* axes, the errors can be partially suppressed, but the errors caused by rounding can still not be completely eliminated. Therefore, it is suggested that when focal mechanism solutions are published, complete focal mechanism solution information (including six parameters of two seismic nodal planes and six other parameters, i.e., plunges and azimuths of *T*, *B* and *P* axes) should be published as much as possible; if the intuitive property is neglected, it is allowed to publish the information in the form of seismic moment tensor, or by trying to use three Euler angles in

place of the plunges and azimuths of T, B and P axes, so that subsequent researchers can obtain relatively complete and accurate focal mechanism information.

Acknowledgments We appreciate the constructive comments from two reviewers. This study is supported by Special Foundation for Seismic Research (Grant No. 201208006), Director Foundation of Institute of Seismology, China Earthquake Adminstration (Grant Nos. IS201116013, IS201506220), and National Natural Science Foundation of China (Grant Nos. 40974012, 41304019). The earthquake focal mechanism solution data were collected from the Global CMT (http://www.globalcmt.org/CMTsearch.html).

References

Aki K, Richards PG (1980) Quantitative seismology: theory and methods. University Science Books, San Francisco, pp 41–131

Arnold R, Townend J (2007) A Bayesian approach to estimating tectonic stress from seismological data. Geophys J Int 170:1336–1356. doi:10.1111/j.1365-246X.2007.03485.x

Dreger DS, Helmberger DV (1990) Broadband modeling of local earthquakes. Bull Seismol Soc Am 80(5):1162–1179

Dreger DS, Helmberger DV (1993) Determination of source parameters at regional distances with three-component sparse network data. J Geophys Res: Solid Earth 98(B5):8107–8125. doi:10.1029/93JB00023

Ekström G (1989) A very broad band inversion method for the recovery of earthquake source parameters. Tectonophysics 166(1):73–100. doi:10.1016/0040-1951(89)90206-0

Gao B, Jia K, Zhou SY (2016) Research of locations and source parameters of historical earthquakes equal and greater than M5.0 from 1900 to 1970 in North China. Chin J Geophys 59(11):4089–4099. doi:10.6038/cjg20161113 (in Chinese with English abstract)

Gasperini P, Vannucci G (2003) FPSPACK: a package of FORTRAN subroutines to manage earthquake focal mechanism data. Comput Geosci 29:893–901. doi:10.1016/S0098-3004(03)00096-7

Gephart JW (1990) Stress and the direction of slip on fault planes. Tectonics 9:845–858. doi:10.1029/TC009i004p00845

Gephart JW, Forsyth DW (1984) An improved method for determining the regional stress tensor using earthquake focal mechanism data: application to the San Fernando earthquake sequence. J Geophys Res 89:9305–9320. doi:10.1029/JB089iB11p09305

Hardebeck JL, Shearer PM (2002) A new method for determining first-motion focal mechanisms. Bull Seismol Soc Am 92:2264–2276. doi:10.1785/0120010200

Jost MU, Herrmann RB (1989) A student's guide to and review of moment tensors. Seismol Res Lett 60:37–57. doi:10.1785/gssrl.60.2.37

Kagan YY (2007) Simplified algorithms for calculating double-couple rotation. Geophys J Int 171(1):411–418. doi:10.1111/j.1365-246X.2007.03538.x

Kanamori H, Given JW (1981) Use of long-period surface waves for rapid determination of earthquake-source parameters. Phys Earth Planet Inter 27(1):8–31

Kisslinger C, Bowman JR, Koch K (1981) Procedures for computing focal mechanisms from local (SV/P)z data. Bull Seismol Soc Am 71:1719–1729

Knopoff L, Randall MJ (1970) The compensated linear-vector dipole: a possible mechanism for deep earthquakes. J Geophys Res 75:4957–4963. doi:10.1029/JB075i026p04957

Krieger L, Heimann S (2012) MoPaD—moment tensor plotting and decomposition: a tool for graphical and numerical analysis of seismic moment tensors. Seismol Res Lett 83(3):589–595

Li HJ (1993) Problems and standardization in description of source mechanism. Recent Dev Wold Seismol 11:1–3 (in Chinese with English abstract)

Ma ST, Yao ZX, Ji C (1999) To estimate focal mechanisms of moderate earthquakes using a long period surface waveform fitting method as well as first motion signs of P waves. Chin J Geophys 42(06):785–799 (in Chinese with English abstract)

Martínez-Garzón P, Bohnhoff M, Kwiatek G, Dresen G (2013) Stress tensor changes related to fluid injection at the Geysers geothermal field, California. Geophys Res Lett 40:2596–2601. doi:10.1002/grl.50438

Ni JC, Chen YT, Chen XX (1991) Seismic moment tensor and its inversion. Seismol Geomagn Obs Res 5:1–17 (in Chinese with English abstract)

Okamoto T (2002) Full waveform moment tensor inversion by reciprocal finite difference Green's function. Earth Planet Spa 54(6):715–720. doi:10.1186/BF03351723

Reasenberg P, Oppenheimer DH (1985) FPFIT, FPPLOT and FPPAGE; Fortran computer programs for calculating and displaying earthquake fault-plane solutions. US Geol Surv 109:85–739

Sheng SZ, Wan YG, Huang JC, Pu YF, Li X (2015) Present tectonic stress field in the Circum-Ordos region deduced from composite focal mechanism method. Chin J Geophys 58(2):436–452. doi:10.6038/cjg20150208 (in Chinese with English abstract)

Snoke JA (2003) Focmec: focal mechanism determinations. Int Geophys 81:1629–1630

Snoke JA, Munsey JW, Teague AG, Bollinger GA (1984) A program for focal mechanism determination by combined use of polarity and SV-P amplitude ratio data. Earthq Notes 55(3):15

Tan K, Zhao B, Zhang CH, Du RL, Wang Q, Huang Y, Zhang R, Qiao XJ (2016) Rupture models of the Nepal M_W 7.9 earthqauke and M_W 7.3 aftershock constrained by GPS and InSAR coseismic deformations. Chin J Geophys 59(6):2080–2093. doi:10.6038/cjg20160614 (in Chinese with English abstract)

Tape W, Tape C (2012) A geometric setting for moment tensors. Geophys J Int 190(1):476–498. doi:10.1111/j.1365-246X.2012.05491.x

Wan YG (2015) A grid search method for determination of tectonic stress tensor using qualitative and quantitative data of active faults and its application to the Urumqi area. Chin J Geophys 58:3144–3156. doi:10.6038/cjg20150911 (in Chinese with English abstract)

Wan YG (2016) Introduction to seismology. Science Press, Beijing, pp 343–454

Wan YG, Wu ZL, Zhou GW, Huang J (2000) How to get rakes from known strikes and dips of the two nodal planes. Seismol Geomagn Obs Res 21:26–30 (in Chinese with English abstract)

Wang PW (2012) China earthquake case focal mechanism solutions of the specification detection. Earthquake Research Institute of China Earthquake Administration, Wuhan, pp 5–38

Wang F, Cao XB, Zhang SJ (2008) The service in-orbit spacecraft attitude tracking algorithm based on Euler's rotation. J Astronaut 29:570–575 (in Chinese with English abstract)

Wéber Z (2006) Probabilistic local waveform inversion for moment tensor and hypocentral location. Geophys J Int 165(2):607–621. doi:10.1111/j.1365-246X.2006.02934.x

Yi GX, Long F, Amaury V, Yann K, Liang MJ, Wang SW (2016) Focal mechanism and tectonic deformation in the seismogenic area of the 2013 Lushan earthquake sequence, southwestern China. Chin J Geophys 59(10):3711–3731. doi:10.6038/cjg20161017 (in Chinese with English abstract)

Yue H, Lay T (2013) Source rupture models for the M_W 9.0 2011 Tohoku Earthquake from joint inversions of high-rate geodetic and seismic data. Bull Seismol Soc Am 103(2B):1242–1255. doi:10.1785/0120120119

Zhang LF, Fatchurochman I, Liao WL, Li JG, Wang QL (2013) Source rupture process inversion of the 2013 Lushan earthquake, China. Geod Geodyn 4(2):16–21. doi:10.3724/SP.J.1246.2013.02016

Zhang LF, Li JG, Liao WL, Wang QL (2016) Source rupture process of the 2015 Gorkha, Nepal M_W 7.9 earthquake and its tectonic implications. Geod Geodyn 7(2):124–131. doi:10.1016/j.geog.2016.03.001

Zhu L, Rivera LA (2002) A note on the dynamic and static displacements from a point source in multilayered media. Geophys J Int 148:619–627. doi:10.1046/j.1365-246X.2002.01610.x

Zhu LM, Wu XP, Li JW, Wu X (2010) Euler's rotation transform and dynamic equations of a rectangular coordinate system. Hydrogr Surv Charting 30:20–22